



## INDUSTRIAL ROBOT CALIBRATION USING A VIRTUAL LINEAR CONSTRAINT

Biqiang Du <sup>1\*</sup>, Ning Xi <sup>2</sup>, Erick Nieves <sup>2</sup>

<sup>1</sup> Department of Mechanical Engineering, North China Electric Power University, Baoding,  
071003, China

<sup>2</sup> Department of Electrical and Computer Engineering, Michigan State University, East Lansing,  
MI 48824, USA

\* Corresponding author: Ncepudu@gmail.com

---

*Submitted: Aug.19, 2012*

*Accepted: Oct.25, 2012*

*Published: Dec.1, 2012*

---

*Abstract- This paper proposes a systematic method to identify the joint zero offset of industrial robot. Small offset always exist in robot joint, which affect the precision in kinematic equations leading to calculate wrong joint angle values. To solve these problems, the proposed method employs a portable dual Position Sensitive Detector (PSD) device and a focusable laser point (FLP). The portable dual PSD device comprises two fixed PSDs tilted in an angle to reflect the laser line from one PSD to another. The FLP, attached to the robot end-effector, aims at both centers of the two PSDs at the same time, effectively creating a virtual linear constraint for the robot end-effector. As a result, small variations in position and orientation of the end-effector are magnified on the laser spot's location at the PSD's surface. Hence, the resolution of measuring the position and orientation of the end-effector*

*is improved due to the high precision feedback of the PSD, increasing the accuracy of joint angle measurements that are required to calibrate the robot. From the easily measured joint angle readings, and an identification model, the joint zero offset of industrial robot is calibrated. The effectiveness and accuracy of the method are verified using both simulations and real experiments on an IRB120 robot.*

**Index terms:** Industrial robot, robot calibration, zero offset, portable dual PSD device, laser point.

## I. INTRODUCTION

Nowadays, modern production needs more complex process which makes great improvement for industrial robots. The improvement depends on two important features inherent to industrial robots: repeatability and accuracy. Typically, industrial robots attain high repeatability levels and are able to successfully perform their tasks because they are mainly used in repetitive applications. These repeatability values clearly demonstrate the high mechanical quality of these manipulators and their precise positioning capacities. In these cases, repeatability of a robot is all that matters and the accuracy is not important. However, in the offline programming, accuracy is a significant concern. Unfortunately, Experience has shown that industrial robots have much lower accuracy than repeatability [1]. Hence, different methods for robot accuracy enhancements have been shown in extensive literatures, especially for industrial robots.

Although there are several sources of inaccuracy, (e.g. thermal expansion, gear errors, structural deformations, or even incorrect knowledge of link and joint parameters) the main source of inaccuracy lies in kinematic model parameter errors. It has been shown that as much as 95% of robot positioning inaccuracy arises from the inaccuracy in its kinematics model description [2]. As we know, the majority of the kinematic parameters, (e.g. arm length, link offset, and link twist angles) are related to the structural mechanics of the manipulator. Typically, these parameters do not change too much after the robot is shipped and installed in the manufacturing areas. However, some kinematics parameters such as zero offset might be affected by the assembly or the replacement of motor and encoder. In this situation, the kinematic calibration, also called geometric calibration, is used to improve the position and orientation accuracy of the industrial robot by identifying inaccurate and unknown kinematic model parameters that either minimize the error caused by the manipulator or better fit the robot's actual kinematics. Indeed, numerous

robot kinematics parameters calibration systems and methodologies have been developed in both academia and industry.

Of the large number of robot calibration techniques documented in the literature (in terms of measurement systems used in data capture, constraints, or sequencing data sampling and later treatment [3]), it is possible to classify them as two types: (1) open-loop methods and (2) closed-loop methods. Open-loop methods involve measuring the real end-effector pose, which requires special external measuring devices (such as theodolites [4], inclinometers [5], Computer Numerical Controlled (CNC) machines [6], Coordinate Measuring Machines [7], and laser tracking system [8, 9]). Due to the fact that such equipments are certainly not much more affordable (a laser tracker still costs more than \$100,000) or their procedures are time consuming, they are difficult to be used extensively in the manufacturing plants.

Closed-loop methods are based on a closed kinematic chain by fix one or more of the position and orientation constraints to the end-effector. This allows the establishment of an equation system to determine a set of parameters, which is known as a self-calibration technique. As much in the literature as in practice, closed-loop methods are more widespread and have received much more attentions because an external measuring device is not necessary. Ikits *et al.* [10] and Zhuang *et al.* [11] imposed plane constraints on the end-effector positions. Alberto *et al.* [12] measured the poses of a robot by matching the pin of the end-effector to a hole on a dime. Meggiolaro *et al.* [13] used a single endpoint contact constraint, equivalent to a ball joint. The robot moves to different configurations that satisfy the physical contact constraint. These methods are problematic because they need some external physical contact constraints and suffer from their manufacturing accuracies.

To solve the problem, some methods based on an uncontract constraint have been proposed. Unlike previous closed-loop methods, these approaches do not require any physical constraints. Newman *et al.* [14] and Chen *et al.* [15] used a laser line as a virtual linear constraint on the end-effector positions allowing the end effector to slide along a line. Gatla *et al.* [16] proposed a new method called “virtual closed kinematic chain”. In their method, a laser pointer tool, attached to the end-effector, aims at a constant but unknown location on a fixed distant object, effectively creating a virtual closed kinematic chain. However the coincidence of the end-effector position with the line or point is judged by the operator.

Among the existing robot calibration methods, the optical approach using Position Sensitive Detector (PSD) for robot calibration is one of the best choices since it promises high precision, fast response, and a low computational load. Liu et al. [17] described a virtual line-based single-point constraint approach. This approach relies mainly upon a laser pointer attached on the end-effector and single PSD arbitrarily located on the work cell. By aiming the laser lines at the center of the PSD surface with seven different robot configurations at least, various sets of robot joint angles can be recorded. Simulation and experiment showed that the zero offset can be estimated based on these recorded angles. However, the method is time-consuming and its effect is related to the robot configuration.

In this paper, we propose a systematic virtual linear constraint method for industrial robot zero offset calibration. The developed method employs a focusable laser point (FLP) and a portable dual PSD device. The portable dual PSD device comprises of two fixed PSDs tilted in an angle to reflect the laser line from one PSD to another. To implement the developed method, the FLP, attached at the robot end-effector, aims the laser beam at the center of PSD1 and the laser beam is reflected off the PSD1 surface with a direction towards the center of PSD2. Then we can get a line which pass through the centers of both PSDs. Its reflect line is the virtual linear constraint in our method, which means that the robot end-effector, together with the laser point, are constrained to move along the reflect line. The portable dual PSD device is arbitrarily located, so its position and orientation with respect to the robot are unknown. During the whole calibration process, the procedure of aiming the laser beam at both centers of the two PSDs only repeats three times, so the approach is simpler and less time consuming. Once the above process has been done, various sets of robot joint angles will be recorded. Based on the recorded joint angles and robot forward kinematics, a robot calibration method is developed. In terms of the mathematic solution of the procedure, our proposed method also uses non-linear, iterative optimization techniques to identify the robot calibration parameters from the data that is recorded from different mechanism positions and orientations; this process helps minimize the error. We select the traditional Gauss-Newton nonlinear least squares method [18] to solve the optimization problem and identify the zero offset. Both simulations and experiments on an ABB IRB120 industrial robot were implemented to verify the efficiency and accuracy of the proposed method as well as the feasibility of the newly developed calibration system.

This paper is organized as follows. Section II describes the new zero offset calibration methodology and its system model. Sections III and IV present the simulation results and the experimental results on an IRB120 industrial robot, respectively, to verify the effectiveness and the accuracy of the proposed calibration method. Our conclusions are presented in Section V.

## II. CALIBRATION METHODOLOGY

### a. Calibration system model

Figure 1 shows the schematic model of robot offset calibration system, which mainly consists of a robot, a laser and adapter, a portable dual PSD device.

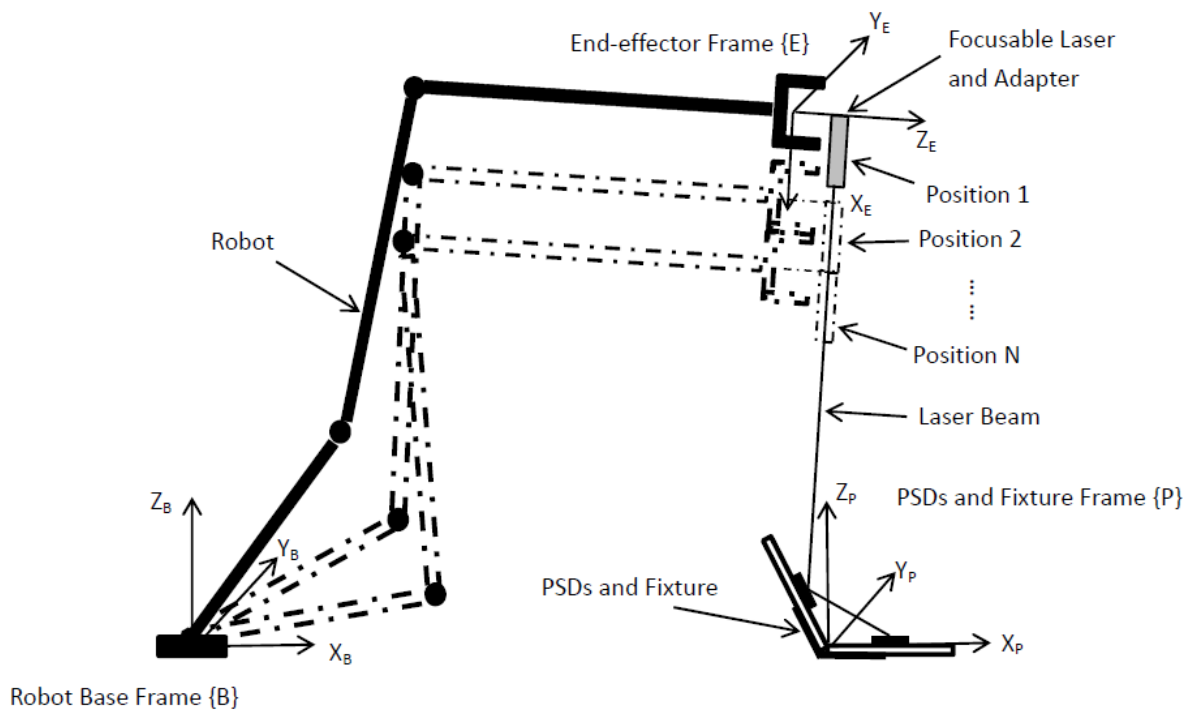


Figure 1. Model of robot offset calibration system

The robot is modeled from a 6-DOF (Degrees Of Freedom) industrial robot. A focusable laser pointer with its adapter is mounted and rigidly fixed on the robot end-effector. The laser beam is adjusted to align its orientation toward the X-axis of the End-effector frame  $\{E\}$ . Two PSDs are arbitrarily located on a fixture. The location of fixture with respect to the Robot base frame  $\{B\}$  is also arbitrary and unknown. We adopt the segmented PSD for its high precision feedback. The

segmented PSD has a higher resolution than  $0.1\mu\text{m}$  in theory. Even under the experimental condition, its resolution may reach approximately  $2\mu\text{m}$  [19].

#### b. Analysis of kinematics error model

The first part of any calibration process is to define a kinematic model for the robot. The kinematic parameters of the robot can then be set according to the selected model. For the robot model with  $n$  ( $n=6$ ) joints as shown in Figure 1, the forward kinematics can be represented by the following equation,

$${}^B T_E = \prod_{i=1}^n A_i \quad (1)$$

where  ${}^B T_E$  is the transformation matrix that expresses the position and orientation of the robot end-effector frame  $\{E\}$  with respect to the robot base frame  $\{B\}$ ;  $A_i$  is the homogeneous transformation matrix associated with link  $i$  and joint  $i$ .

Commonly kinematic model method is the D-H parameters defined by Denavit-Hartenberg. It models the relationship between two consecutive link coordinate frames with four parameters. By Denavit-Hartenberg (D-H) model, each homogeneous transformation matrix  $A_i$  can be written as

$$A_i = \begin{bmatrix} c\theta_i & -s\theta_i c\alpha_i & s\theta_i s\alpha_i & a_i c\theta_i \\ s\theta_i & c\theta_i c\alpha_i & -c\theta_i s\alpha_i & a_i s\theta_i \\ 0 & s\alpha_i & c\alpha_i & d_i \\ 0 & 0 & 0 & 1 \end{bmatrix} \quad (2)$$

where the four quantities  $a_i$ ,  $\alpha_i$ ,  $d_i$ , and  $\theta_i$ , denotes the link length, link twist, link offset, and joint angle, respectively.  $c\theta_i$  denotes  $\cos\theta_i$  while  $s\theta_i$  denotes  $\sin\theta_i$ .

We can use the same model to include the zero offset of each joint as follows; let  $\delta_i$  denotes the offset value of the joint  $i$ , then each homogeneous transformation can be rewritten as,

$$A'_i = \begin{bmatrix} c\theta'_i & -s\theta'_i c\alpha_i & s\theta'_i s\alpha_i & a_i c\theta'_i \\ s\theta'_i & c\theta'_i c\alpha_i & -c\theta'_i s\alpha_i & a_i s\theta'_i \\ 0 & s\alpha_i & c\alpha_i & d_i \\ 0 & 0 & 0 & 1 \end{bmatrix} \quad (3)$$

where  $s\theta'_i$  denotes  $\sin(\theta_i + \delta_i)$  and  $c\theta'_i$  denotes  $\cos(\theta_i + \delta_i)$ .

Combining the zero offset and substituting (3) into (1), forward kinematics  ${}^B T_E$  with the offset is written as,

$${}^B T_E = \begin{bmatrix} T_{11} & T_{12} & T_{13} & T_{14} \\ T_{21} & T_{22} & T_{23} & T_{24} \\ T_{31} & T_{32} & T_{33} & T_{34} \\ 0 & 0 & 0 & 1 \end{bmatrix} = \prod_{i=1}^6 \tilde{A}_i = \tilde{A}_1 \tilde{A}_2 \tilde{A}_3 \tilde{A}_4 \tilde{A}_5 \tilde{A}_6 \quad (4)$$

Note that joint 1 is dependent on the robot base frame  $\{B\}$ . So in (4), there are five unknown parameters, *i.e.*, the last five offsets  $\delta_i (i = 2, 3, \dots, 6)$ .

### c. Zero offset calibration

The calibration procedure, as shown in figure 1, is performed by locating the end-effector and the laser pointer several times at different positions. However, no matter where the laser pointer is, the laser beam should always aim at both centers of two PSDs at the same time. Hence,  $N$  ( $N$  is the repeat times of locating) sets of robot joint angles can be recorded from robot controller.

Because the laser pointer is rigidly fixed on the robot end-effector, we denote the  $j$ th position of the laser pointer as  $P_j = [P_{xj}, P_{yj}, P_{zj}]^T (j = 1, 2, \dots, N)$  and the unit direction vector of the laser line direction as  $[m_j, n_j, p_j]^T$ . Replacing the recorded joint angles into the forward kinematics equation (4), we can decompose them as follows,

$$\begin{bmatrix} m_j \\ n_j \\ p_j \\ 0 \end{bmatrix} = ({}^B T_E)_j \begin{bmatrix} 1 \\ 0 \\ 0 \\ 0 \end{bmatrix} = \begin{bmatrix} T_{11} \\ T_{21} \\ T_{31} \\ 0 \end{bmatrix}_j, \quad j = 1, 2, \dots, N \quad (5)$$

$$\begin{bmatrix} P_{xj} \\ P_{yj} \\ P_{zj} \\ 1 \end{bmatrix} = ({}^B T_E)_j \begin{bmatrix} 0 \\ 0 \\ 0 \\ 1 \end{bmatrix} = \begin{bmatrix} T_{14} \\ T_{24} \\ T_{34} \\ 1 \end{bmatrix}_j, \quad j = 1, 2, \dots, N \quad (6)$$

Because all these positions  $P_j (j = 1, 2, \dots, N)$  are in the same virtual line, they have following relationships,

$$\left\{ \begin{array}{l} m_1 = m_j \\ n_1 = n_j \\ p_1 = p_j \\ \frac{P_{x1} - P_{xj}}{m_1} = \frac{P_{y1} - P_{yj}}{n_1} = \frac{P_{z1} - P_{zj}}{p_1} \end{array} \right., \quad j \neq 1 \quad (7)$$

Hence, for  $j$ th ( $j \neq 1$ ) position of the laser pointer, we has a squared error

$$\psi_j = \psi_{j1}^2 + \psi_{j2}^2 + \psi_{j3}^2 + \psi_{j4}^2, \quad j \neq 1 \quad (8)$$

where

$$\psi_{j1} = (T_{11})_j - (T_{11})_1 \quad (9)$$

$$\psi_{j2} = (T_{21})_j - (T_{21})_1 \quad (10)$$

$$\psi_{j3} = \frac{(T_{11})_1}{(T_{21})_1} - \frac{(T_{14})_j - (T_{14})_1}{(T_{24})_j - (T_{24})_1} \quad (11)$$

$$\psi_{j4} = \frac{(T_{21})_1}{(T_{31})_1} - \frac{(T_{24})_j - (T_{24})_1}{(T_{34})_j - (T_{34})_1} \quad (12)$$

Hence the unknown parameters, *i.e.*, the last five zero offsets  $\delta_i$  ( $i = 2, 3, \dots, 6$ ), are identified by minimizing the total sum of the squared error.

$$\Psi = \arg \min \sum_{j=2}^N \psi_j \quad (13)$$

Since this is a quite complicated optimization problem with 5 parameters, at least 3 sets of robot joint angles are essential, *i.e.*,  $N \geq 3$ . The Gauss-Newton nonlinear least squares method will be used to minimize the total sum of the squared errors.

### III. CALIBRATION WITH PRECISE DATA IN SIMULATION

The MATLAB simulations of the calibration experiment were performed as a proof of concept. An ABB IRB120 robot was modeled using its coordinate frames definition (see figure 2) and D-H parameters (see Table 1).



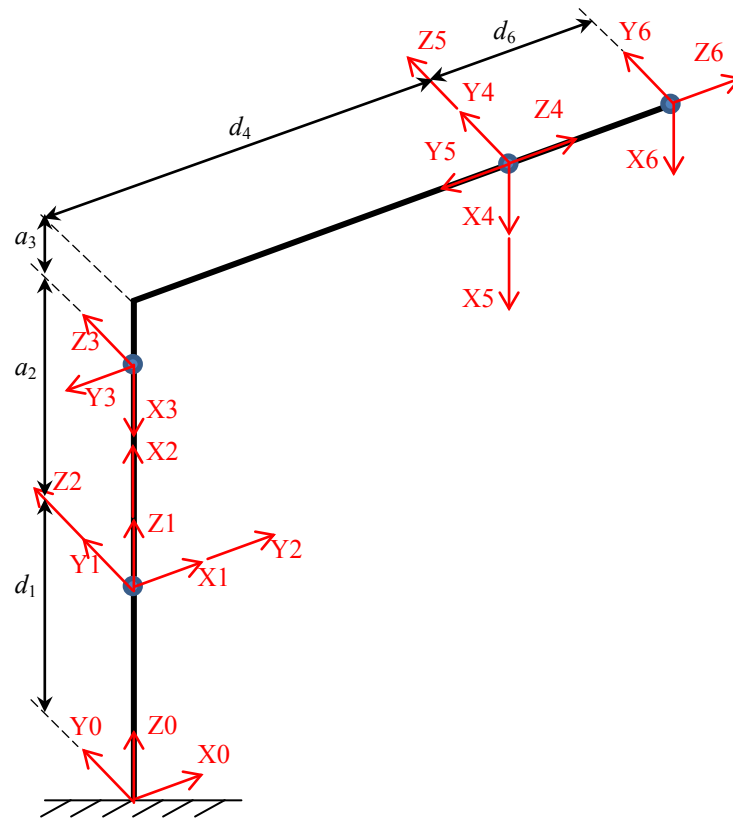


Figure 2. Coordinate frames defined for ABB IRB120 robot

Table 1: D-H parameters of the ABB IRB120 robot

Joint	$a$ (mm)	$\alpha$ ( $^{\circ}$ )	$d$ (mm)	$\theta$ ( $^{\circ}$ )	Range ( $^{\circ}$ )
1	0	-90	290	0	-165 to 165
2	270	0	0	-90	-110 to 110
3	-70	90	0	180	-90 to 70
4	0	-90	302	0	-160 to 160
5	0	90	0	0	-120 to 120
6	0	0	75	0	-400 to 400

In the simulations the laser pointer was attached on the end-effector to align the laser line with the X-axis of the robot end-effector frame, the same way we did for the experimental system design. A virtual PSD feedback device was also built and used to accurately aim the laser beam at the center of PSD, so that the simulations could find various robot configurations along the

virtual linear constraint. Simulations of the zero offset calibration were performed using initial zero offset parameters, which means that we synthesize offset values for each joint in the kinematic model and compare them with the values our proposed method identified. The simulations were implemented by locating the robot at seven different configurations. Seven corresponding sets of joint angles were recorded from the robot controller (see Table 2), so that the calibration parameters could be identified by the proposed method with  $N = 3, 4, 5, 6$  or  $7$ .

Table 2: Robot joint angles recoded from seven different configurations

Configuration	Joint angle (°)					
	1	2	3	4	5	6
1	-16.28	18.99	38.13	130.79	86.98	-163.13
2	-16.85	14.95	38.85	130.13	85.07	-160.39
3	-17.45	11.04	39.28	129.36	83.13	-157.46
4	-18.06	7.29	39.40	128.48	81.17	-154.35
5	-18.71	3.74	39.21	127.46	79.22	-151.08
6	-19.38	0.41	38.73	126.33	77.34	-147.65
7	-20.08	-2.67	37.94	125.07	75.54	-144.09

In Table 3, the results of the calibration simulations together with the deviations relative to synthetic offset values are shown. Column 2 shows the synthetically generated offset parameters. Column 3 shows the initial parameters used in the Gauss-Newton minimization routine. Column 4 shows the identified offsets and column 5 shows the standard deviations of the parameters from the synthetic offset values. Because the identified offsets did not make any difference with different number of configurations ( $N$ ), we only shows the results with  $N=3$ . The results show that the offsets identified by the calibration simulations were exactly equal to the synthetic values, which indicates the stability and effectiveness of the method.

In the minimization routine, no matter how many different configurations were introduced, the solution can be obtained with error residue less than  $1e-12$  within the first three iterations. The procedure is continued to show the convergence.

Table 3: Simulation results on joint offset calibration from three different configurations

Parameter	Synthetic (°)	Initial (°)	Identified (°)	Deviation
$\delta_2$	1.20	0.00	1.20	0.00
$\delta_3$	0.80	0.00	0.80	0.00
$\delta_4$	-1.40	0.00	-1.40	0.00
$\delta_5$	-0.60	0.00	-0.60	0.00
$\delta_6$	-1.00	0.00	-1.00	0.00

#### IV. EXPERIMENTAL ANALYSES

##### a. Calibration of IRB120 robot

The calibration experiment was performed on a real IRB120 robot as shown in Figure 3. The locations of laser spot at both PSDs were wirelessly [20, 21] transferred to the computer.



Figure 3. ABB IRB120 robot and the proposed calibration system

The experiment was repeated multiple times with different positions of the portable dual PSD device, and the identified parameters resulting from these calibrations (which should all be the

same) were compared by computing the mean and deviations of the parameters. Using various positions of the portable dual PSD device, and conducting the experiment ensures that the parameters obtained were stable and accurate.

Table 4: Calibration results on a real IRB120 robot

Parameter	Initial	Case 1	Case 2	Case 3	Case 4	Case 5	Case 6	Mean	STD ( $\times 10^{-3}$ )
$\delta_2$ (°)	0	2.0303	2.0527	1.8455	1.9908	1.9474	1.8044	1.9452	1.756
$\delta_3$ (°)	0	0.5546	0.5080	0.6100	0.5566	0.4658	0.6041	0.5498	0.970
$\delta_4$ (°)	0	-0.2045	-0.1939	-0.2141	-0.1718	-0.1929	-0.1884	-0.1926	0.211
$\delta_5$ (°)	0	-0.0910	-0.0930	-0.1374	-0.0929	-0.0961	-0.0932	-0.1006	0.316
$\delta_6$ (°)	0	-0.2384	-0.2324	-0.2391	-0.2644	-0.2279	-0.2544	-0.2428	0.242

Table 4 shows the results of the calibration of the real robot. Column 2 shows the initial parameters used in the Gauss-Newton minimization routine, i.e., the industrial model parameters provided by the factory controller. Column 3~8 show the identified parameters from multiple trials. Column 9 shows the mean value of the parameters and column 10 shows the standard deviation of the parameters from multiple trials. The standard deviation of the solution was small ( $10^{-3}$ ) indicating the stability of the procedure. The accuracy of the obtained solution is discussed as follows.

#### b. Accuracy of IRB120 robot

To test the accuracy of the calibration procedure, the portable dual PSD device was located at a fixed position and the laser line was aligned to hit the center of both PSDs using various robot configurations. The accurate positions of robot end-effector were computed for each configuration using calibrated parameters. These positions usually do not locate at a common line. Therefore, a common closest line which is closest to all the positions was found. The projections of all the positions onto a plane normal to this common closest line were plotted. The larger the error in the parameters, the greater will be the scattering in the projected positions.

The errors in the projection using calibrated parameters for real robot are shown in figure 4. Since the robot was aiming at the same point from various robot configurations, all of the

projected points should be coincident. The spread of these projected points relates to the accuracy of the calibrated parameters of the robot. Figure 4 shows that the spread of projected positions. The standard deviation of the radius of spread was only  $14.2\mu\text{m}$ . Therefore we can also claim that an accurate joint offset calibration results can be received by our new dual PSD methodology.

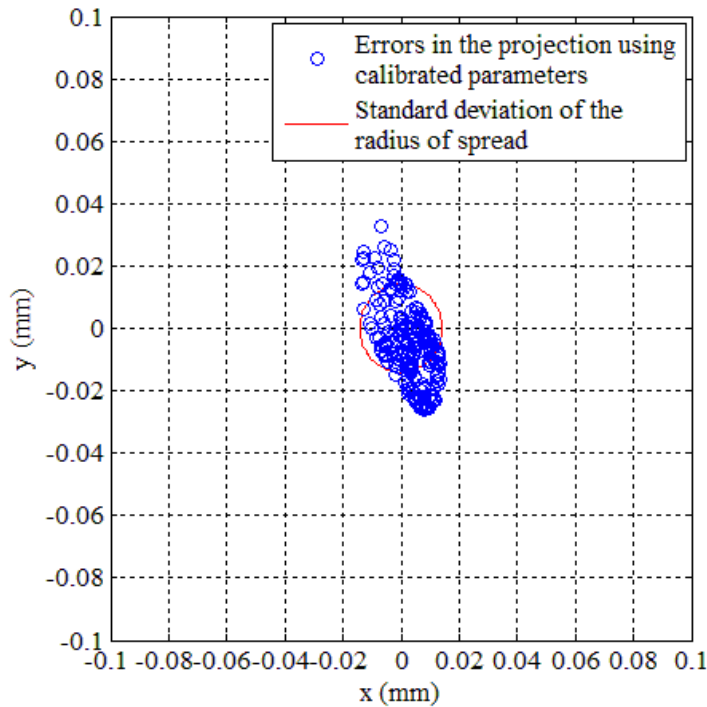


Figure 4. Deviations using calibrated parameters for IRB120 robot

## V. CONCLUSIONS

An effective and accurate calibration method is developed for industrial robots. Most of the previous methods that calibrate a robot use the pose of the end effector measured by some external equipment. The accuracy of measurements of the end-effector's position and orientation is limited by the measuring equipment and its resolution. Other closed-loop methods using physical constraints, such as linear, planar, or other endpoint constraints are difficult in maintaining the end-effector constraints, or limited by the manufacturing accuracy of constraints. The proposed method uses a focusable laser point, attached on the robot's end effector, to aim at a portable dual PSD device. By projecting the laser point onto the both centers of two PSDs at the

same time, the method limits the robot end-effector to a virtual linear constraint. Due to the high precision feedback of PSD, the resolution of observations is improved, increasing the accuracy of measurements of the joint angles required for accurate calibration of the robot. The method is verified using both simulations and real experiments on an IRB120 industrial robot.

## ACKNOWLEDGMENTS

This work was supported by Fundamental Research Funds for the Central Universities under Grant No. 10QG12.

## REFERENCES

- [1] B. Mooring, Z. S. Roth and M. R. Driels, *Fundamentals of manipulator calibration*, John Wiley & Sons, 1991.
- [2] X. L. Zhong and J. M. Lewis, "A new method for autonomous robot calibration", *Proceedings of the 1995 IEEE International Conference on Robotics and Automation*. Nagoya, Aichi, Japan, 1995, pp.1790-1795.
- [3] J. M. Hollerbach and C. W. Wampler, "The calibration index and taxonomy for robot kinematic calibration methods", *International Journal of Robotics Research*, Vol.15, No.6, 1996, pp.573–91.
- [4] M. R. Driels and U. S. Pathre, "Robot calibration using an automatic theodolite", *The International Journal of Advanced Manufacturing Technology*, Vol.9, No.2, 1994, pp.114-125.
- [5] A. Rauf, A. Pervez and J. Ryu, "Experimental results on kinematic calibration of parallel manipulators using a partial pose measurement device", *IEEE Transactions on Robotics*, Vol.22, No.2, 2006, pp.379-384.
- [6] J. H. Borm and C. H. Meng, "Determination of optimal measurement configurations for robot calibration based on observability measure", *The International Journal of Robotics Research*, Vol.10, No.1, 1991, pp.51-63.
- [7] M. R. Driels, W. Swayze and S. Potter, "Full-pose calibration of a robot manipulator using a coordinate-measuring machine", *The International Journal of Advanced Manufacturing Technology*, Vol.8, No.1, 1993, pp.34-41.
- [8] K. Lau, R. J. Hocken and W. C. Haight, "Automatic laser tracking interferometer system for robot metrology", *Precision Engineering*, Vol.8, No.1, 1986, pp.3-8.
- [9] A. Nubiola and I. A. Bonev, "Absolute calibration of an ABB IRB1600 robot using a laser tracker", *Robotics and Computer-Integrated Manufacturing*, Vol.29, No.1, 2013, pp.236-245.

- [10] M. Ikits and J. M. Hollerbach, "Kinematic calibration using a plane constraint", Proceedings of the 1997 IEEE International Conference on Robotics and Automation, Albuquerque, NM, USA, 1997, pp.3191–3196.
- [11] H. Zhuang, S. H. Motaghedi and Z. S. Roth, "Robot calibration with planar constraints", Proceedings of the 1999 IEEE International Conference on Robotics and Automation, Detroit, MI, USA, 1999, pp.805–810.
- [12] A. Omodei, G. Legnani and R. adamini, "Calibration of a measuring robot: Experimental results on a 5 DOF structure", Journal of Robotic Systems, Vol.18, No.5, 2001, pp.237-250.
- [13] M. A. Meggiolaro, G. Scriffignano and S. Dubowsky, "Manipulator calibration using a single endpoint contact constraint", Proceedings of the 2000 ASME Design Engineering Technical Conference, Baltimore, MD, USA, 2000, pp.1-8.
- [14] W. S. Newman, C. E. Birkhimer, R. J. Horning and A. T. Wilkey, "Calibration of a Motoman P8 robot based on laser tracking", Proceedings of the Proceedings of the 2000 IEEE International Conference on Robotics and Automation, San Francisco, CA , USA, 2000, pp.3597-3602.
- [15] H. Chen, T. Fuhlbrigge, S. Choi, J. Wang and X. Li, "Practical industrial robot zero offset calibration", Proceedings of the 4th IEEE Conference on Automation Science and Engineering, Washington DC, USA, 2008, pp.516-521.
- [16] C. S. Gatla, R. Lumia, J. Wood, and G. Starr, "An automated method to calibrate industrial robots using a virtual closed kinematic chain", IEEE Transactions on Robotics, Vol.23, No.6, 2007, pp.1105-1116.
- [17] Y. Liu, N. Xi, G. Zhang, X. Li, H. Chen, C. Zhang, M. J. Jeffery and T. A. Fuhlbrigge, "An automated method to calibrate industrial robot joint offset using virtual line-based single-point constraint approach", Proceedings of the 2009 IEEE/RSJ International Conference on Intelligent Robots and Systems, St. Louis, MO, USA, 2009, pp.715-720.
- [18] A. Bjorck, Numerical methods for least squares problems, Society for Industrial and Applied Mathematics, 1996.
- [19] Y. Liu, N. Xi, J. Zhao, E. Nieves-Rivera, Y. Jia, B. Gao and J. Lu, "Development and sensitivity analysis of a portable calibration system for joint offset of industrial robot", Proceedings of the 2009 IEEE/RSJ International Conference on Intelligent Robots and Systems, St. Louis, MO, USA, 2009, pp.3838-3843.
- [20] V. Iyer, G. R. Murthy and M. B. Srinivas, "Training Data Compression Algorithms and Reliability in Large Wireless Sensor Networks", International Journal on Smart Sensing and Intelligent Systems, Vol.1, No.4, 2008, pp.912-921.
- [21] A.Yousaf, F.A.Khan and Prof. Dr. L.M Reindl, "Wireless Sensing of Open Loop Micro Inductors Using Helmholtz Coil", International Journal on Smart Sensing and Intelligent Systems, Vol.4, No.4, 2011, pp.527-546.